The Role of Dry and Wet Isothermal Annealing Treatment on the Structure and the Mechanical Properties of Isotactic Polypropylene Fibers

Ismail Karacan,[1] Hüseyin Benli[2]

[1]*Department of Textile Engineering, Erciyes University, Turkey*
[2]*Mustafa Çıkrıkçıoğlu Vocational School, Erciyes University, Turkey*

Received 19 March 2011; accepted 23 July 2011
DOI 10.1002/app.35335
Published online 3 November 2011 in Wiley Online Library (wileyonlinelibrary.com).

ABSTRACT: Dry and wet annealing of isotactic polypropylene fibers was carried out under constant length at 120°C in air and in glycerine environments with annealing times ranging from 1 to 30 h. A detailed analysis of the infrared spectrum of samples annealed, especially in air, showed clear evidence of the surface oxidation as indicated by the appearance of oxygen containing functional groups. Annealing was found to lead to an improved structural organization as indicated by the crystallinity, crystallite size, and orientation measurements using X-ray diffraction and infrared spectroscopy methods. Analysis of the X-ray diffraction measurements showed a gradual transformation of metastable smectic phase to a more stable α-monoclinic phase with increasing annealing time. Crystallinity, crystallite size, and orientation measurements performed for the samples annealed in air and in glycerine environments showed no distinct difference. Mechanical properties of the annealed samples were influenced by the annealing environment. Annealing in an air environment resulted in a continuous loss of tensile strength up to the annealing time of 12 h due to an oxidation related chain scission mechanism. On the other hand, annealing in glycerine environment resulted in a continuous and gradual increase of tensile strength without loss of physical form up to the annealing time of 30 h. It is suggested that wet annealing in glycerine environment should be used to obtain improved tensile strength values. © 2011 Wiley Periodicals, Inc. J Appl Polym Sci 124: 3037–3050, 2012

Key words: isotactic polypropylene fiber; dry and wet state annealing; infra-red spectroscopy; X-ray diffraction; density; crystallinity; orientation

INTRODUCTION

In terms of the total synthetic fiber consumption, in volume terms, polypropylene (PP) fiber is the fourth major organic fiber to be produced after polyester, polyamide, and acrylic, but it is already the leading commercial fiber in many applications including textile floor coverings, ready-made clothing, and thermally bonded nonwovens. The progressive improvement of the mechanical properties of PP fibers together with the low density resulted in an extension of application areas outside the traditional textile end-uses. The main growth areas in the utilization of PP fiber have been mainly in the fields of medical, hygiene, industrial, and technical textiles.

During the last few decades, an intense interest has been shown in the structure and properties of PP fiber partly due to its phenomenal success as an important industrial fiber in a wide range of end-uses. Published literature points out to numerous studies on the structure, morphology, mechanical properties in particular tensile strength and toughness, and their relationships with each other. A particular emphasis seems to be placed on the influence of thermal history and tensile deformations on the molecular structure of PP. As already known with other synthetic fibers, the physical structure of PP fiber strongly influences its mechanical properties which is usually controlled by the properties of the initial material and the fiber production parameters.[1,2]

In the last few decades, considerable amount of academic and industrial research and development studies have been carried out with the aim of improving the physical and mechanical properties of PP fibers. In particular, Sheehan and Cole[2] in 1964 showed that PP fibers of high tenacity can be manufactured by optimizing slow drawing of paracrystalline isotactic polypropylene (iPP) with low orientation. In the published literature, it is generally accepted that the hot drawing of as-spun iPP fibers with paracrystalline structures characterized by low orientation can be used to produce fibers with very high tensile strength.[3,4] It is generally accepted that the formation of fibers with paracrystalline structure

Correspondence to: I. Karacan (ismailkaracan@erciyes.edu.tr).

Contract grant sponsor: Scientific Research Projects Unit of Erciyes University; contract grant number: FBA-09-955.

is generally favored by melt-spinning conditions under high cooling rate and low spinline stress.[5] To produce fibers with high tensile strength, a high draw ratio is found to be essential while best results are known to be produced by using two-stage or multi-stage drawing.[3,4]

Earlier investigations[5,6–9] have stressed the importance of melt-spinning conditions on the structure and mechanical properties of the resulting PP fibers. These investigations showed that the structure and properties of fibers can be controlled over a wide range by modifying the production conditions. These investigations were limited to extrusion speeds of less than 1500 m/min. Later studies performed by Shimuzu et al.[10–13] showed the effect of high speed melt-spinning, with take-up speeds ranging from 500 m/min to 7000 m/min. The structure and properties of these melt-spun fibers were reported as a function of take-up speed and the spinning temperature. The effects of annealing of the filaments were also reported. Their results showed that the density and the birefringence initially increase rapidly with increasing take-up speed, but the rate of increase decreases substantially above a critical take-up speed that varies with the extrusion temperature.[12] The filament tensile strength and Young's moduli were reported to increase, while elongation at break decreased, with increasing take-up speeds.

It was shown that the spinnability and the resulting structure and properties of PP fibers can be considerably controlled to a great extent by both the molecular weight (M_w) and the molecular weight distribution (i.e., polydispersity).[14,15] Molecular weight and molecular weight distribution is known to have an important role in the determination of the melt spinning characteristics and the physical properties of the resulting PP fibers. It was argued that[2] a narrow molecular weight distribution of polymer was useful but not essential to manufacture high strength PP fiber. Melt flow index (MFI) or melt flow rate is industrially utilized to obtain polymer characteristics prior to melt-spinning stage. The value of MFI is known to be inversely proportional to the apparent melt viscosity and the end pressure losses, and therefore MFI is commercially used as a rough guide for the evaluation of PP fiber spinnability. MFI values are found to be greatly influenced by both molecular weight and molecular weight distribution.[16]

The effect of isotacticity, ethylene comonomer content, and nucleating agent additions on the structure and properties of melt-spun PP filaments were reported for a series of PPs having similar melt flow rates (MFI = 35 g/10 mins), molecular weights, and molecular weight distributions.[17] It seems that increasing the degree of isotacticity leads to higher crystallinity and tensile modulus of as-spun PP fibers, whereas increasing ethylene comonomer content seems to have the opposite effect.[17] The addition of nucleating agent seems to lead to greater crystallinity, but under certain conditions it is reported that it may lead to reduced tensile modulus. The structure and properties of iPP fibers can be influenced to a greater extent by the postspinning treatments such as annealing or more commonly known as heat treatment.

The annealing treatment can be viewed as a postspinning process in which the polymer structure is subjected to an elevated temperature below the melting point for a specific time followed by cooling to room temperature. The primary purpose of annealing treatment is to release the internal stresses and strains which take place during the melt-spinning stage.[18] The annealing treatment is therefore closely involved with improved dimensional stability, reduction, or elimination of structural defects and enhancement of the physical properties of the polymers. Annealing is known to permit easier rearrangement of polymer chains depending on the temperature used. Hot drawing of the thermoplastic polymers followed by annealing treatment is often employed to enhance the drawing performance. Annealing conditions are known to depend on the temperature, duration, and environmental conditions used during the processing stages.

Farrow[19] proposed that the melting point of iPP can be increased up to 200°C after a suitable annealing treatment at a temperature close to the melting point for long periods provided that the iPP can be made with little or no atactic content. It was shown that the increase in melting point with annealing time was primarily due to an increase in crystallite size rather than the degree of crystallinity. With this approach, a laser heating temperature of 140°C was used for drawing the filaments with a final draw ratio[20] of 51.63. Apart from annealing or heat treatment in an air heated atmosphere, carbon dioxide laser heating systems are reported to be used for the development of ultra-fine PP microfibers.[20,21] It is claimed that laser-heating allows easier fabrication of ultra-thin microfibers compared with the conventional technology such as the conjugate spinning. Laser heating system was also reported to be used for the manufacture of ultra-thin hollow iPP fiber.[22]

Annealing is known to play an important role in manufacturing fibers with enhanced mechanical properties. It seems that zone-drawing and zone-annealing at a temperature close to the melting point can be used to produce high-strength and high-modulus iPP fibers.[23] Mukhopadhyay et al.[24] used gradient heating system at a gradient of 140–140–145°C to produce high modulus and high tenacity PP fibers having an initial modulus of 17.5 GPa and a tenacity

of 750 MPa. This heating system is claimed to allow very high draw ratios of up to 19 with very low void fraction.

The aim of the present study was to characterize and establish the structure–mechanical property relationships of iPP fibers annealed at an isothermal temperature of 120°C in air and in glycerine environments in terms of the degree of crystallinity, crystallite size, and molecular orientation parameters. The structure and properties of the resulting annealed samples were characterized by infrared spectroscopy, X-ray diffraction, and mechanical property measurements.

EXPERIMENTAL DETAILS

Fiber production

The melt-spun as-spun iPP fibers were produced using Barmag® CF melt-spinning machine operating at an extrusion speed of 2500 m/min. Extrusion temperature was set at (235 ± 2)°C. Fiber grade PP granules with weight average molecular weight of 179,000 and polydispersity (M_w/M_n) of 4.6 obtained from Basell Polyolefins with a nominal MFI of 25 g/10 min were used during the fiber extrusion stages. MFI measurements were carried out according to ASTM D1238 using a load for extrusion of 2.16 kg. The melt-extruded filaments were immediately solidified with the assistance of cooling air with a blow speed of 40–70 m/s and a cooling air blow temperature of 18–19°C. During the melt-extrusion stage, a spinnerrette pressure of 60–70 bar and a spinnerrette hole diameter of 200 μm was utilized. The melt-extrusion was performed with environmental conditions having the typical characteristics of 70% relative humidity and 15°C. The original untreated samples were treated with 5% aqueous ethanol solution for 30 min at 50°C to remove the spin finish oil present on the surface of the fibers followed by washing under running water for 30 min to remove the final remains. The samples were wound onto stainless square steel frame with the aim of constraining the samples under constant length to prevent the physical shrinkage and also to prevent the loss of molecular orientation. Annealing was performed in heated air and in glycerine environments at an isothermal temperature of 120°C for soaking times ranging from 1 to 30 h. During the annealing stage, a constant heating rate of 1 °C/min was utilized. After the glycerine treatment, samples were washed twice with hot water, followed by a single warm water washing and finally rinsing under running water for at least 30 min until the samples are free of glycerine. All the samples were finally dried in an air environment for at least 24 h.

X-ray diffraction

The wide-angle X-ray diffraction traces were obtained using a Bruker® AXS D8 Advance X-ray diffractometer system utilizing nickel filtered CuK_α radiation (wavelength of 0.154056 nm) and a voltage and current settings of 40 kV and 40 mA, respectively. Counting was carried out at 10 steps per degree. The observed equatorial X-ray scattering data were collected in the 10–35° 2θ range.

Infra-red spectroscopy measurements

Perkin–Elmer® Spectrum 400 FTIR spectrometer was employed for infrared measurements using single reflection diamond crystal based GladiATR® model ATR attachment. ATR-IR technique is known to be a surface characterization technique and is known to be sensitive to about a few microns into the surface of the samples. In some cases depth of beam penetration can be as much as 1.66 μm at 1000 cm^{-1} for diamond ATR crystals and 0.65 μm at 1000 cm^{-1} for germenium ATR crystals. All the spectra were collected in the mid-IR range (i.e., 4000–400 cm^{-1}) with coadded 50 scans collected at a resolution of 2 cm^{-1}. Finally, all the spectra were analyzed using the OMNIC software® and curve fitting procedures to obtain accurate peak parameters wherever it is necessary.

Mechanical property measurements

Fiber mechanical properties were measured using Zwick-Roell 1446 tensile tester at room temperature. A crosshead speed (stretching rate) of 12.5 mm/min was used for all the experiments. The initial length of the sample was set at 25 mm. Careful attention was taken to minimize stretching and slippage of the filaments before testing and while placing the sample in the grips. Tensile modulus was evaluated from the initial slope of the tensile curve. The elongation and tensile strength at break were determined at the position of break. Reported values were averages of at least 20 tests.

EXPERIMENTAL DATA ANALYSIS

X-ray data-curve fitting

All the X-ray diffraction traces obtained from the annealed iPP samples were fitted with a curve fitting procedure developed by Hindeleh et al.[25] to separate overlapping peaks. Each profile is considered to have the combination of Gaussian and Cauchy functions. When the observed and calculated intensity traces converge to the best acceptable parameters, the computer program provides the list of peak parameters in terms of profile function parameter (f),

peak height, half-height width, and peak position. In the curve fitting program, the profile function parameter also known as peak shape factor is allowed to vary between 0 and 1 and effectively describes the tail region of the profiles. When the profile function parameter (f) is equal to unity, the peak has a Gaussian intensity distribution and when equal to zero, it has a Cauchy shape. Initially, a value of f equal to 0.5 is given to start the fitting process and then the minimization procedure finds the best peak parameters.

Evaluation of the apparent X-ray crystallinity

Apparent X-ray crystallinity (χ_c) is based on the ratio of the integrated intensity under the resolved peaks to the integrated intensity of the total scatter under the experimental trace.[26] This definition can be expressed as in the eq. (1).

$$\chi_c = \frac{\int_0^\infty \mathrm{I_{cr}}(2\theta)d(2\theta)}{\int_0^\infty \mathrm{I_{tot}}(2\theta)d(2\theta)} \quad (1)$$

The area under the background is considered to correspond to the noncrystalline scatter (i.e., amorphous phase). In this work, apparent X-ray crystallinity was estimated in the 2θ range between 10 and 35°.

Evaluation of the apparent crystallite size

Apparent crystallite size measurements were made using the peak parameters obtained from the curve fitting of equatorial X-ray diffraction profiles for the iPP fibers annealed in air and in glycerine environments at an annealing temperature of 120°C for annealing times ranging from 1 to 30 h. Crystallite size calculations usually take into account the broadening imposed by the finite width of the X-ray diffractometer beam. This behavior is reflected as a broadening of the peak width and must be corrected using an appropriate procedure. The peak widths at half-height were corrected using the Stoke's deconvolution procedure.[27] Finally, the apparent crystallite size (L_{hkl}) of a given reflection was calculated using the Scherrer equation:

$$L_{hkl} = \frac{K.\lambda}{\beta.\cos(\theta)} \quad (2)$$

where θ is the Bragg angle for the reflection concerned, λ is the wavelength of radiation (wavelength of 0.154056 nm), L_{hkl} is the mean length of the crystallite perpendicular to the planes (hkl), β is either the integral breadth or the breadth at half maximum intensity in radians, and K is a Scherrer parameter usually taken as 1 for integral breadths and 0.89 for half-widths. Hexamethylene-tetramine compacted at 85°C was used for the instrumental broadening correction.

Infra-red spectroscopy data-curve fitting

In the present work, the parallel and perpendicular polarization spectra were fitted independently, allowing the peak positions and half-height widths to vary freely, using the peak positions previously found using OMNIC® software as a guide to the starting values. Finally, the peak positions and the half-height widths obtained from the two spectra were averaged and the parallel and perpendicular spectra were refitted, fixing the positions and the half-height widths at these average values and allowing only the peak heights to vary.

The infra-red spectrum of iPP in the 1025–775 cm^{-1} region contains at least six well-defined peaks located at 809, 841, 899, 940, 973, and 998 cm^{-1}. During the curve fitting stages, it was necessary to include additional peaks at 796, 827, 852, 886, 931, and 955 cm^{-1} to improve the fits in the tail regions of the major peaks. In the second stage, the IR peak located at 973 cm^{-1} is split into two peaks one at 972 cm^{-1} and the other at 974 cm^{-1}. Curve fitting was restricted to 923–1025 cm^{-1} region for the second stage. Additional peaks needed to improve the fitting are located at 931, 942, 950, 955, and 962 cm^{-1}, respectively. All the IR spectra obtained from the samples were fitted with a curve fitting procedure developed by Hindeleh et al.[25] to separate overlapping peaks.

Evaluation of the infrared crystallinity

Infrared crystallinity was measured by means of the absorbance ratios of the IR bands at 841, 973, and 998 cm^{-1} using the absorbance values obtained during the curve fitting stages. 973 cm^{-1} band has been used as an internal standard due to its presence in the IR spectrum of melted polymer.[28] The absorbance ratios examined in the present investigation are: A_{998}/A_{973} and A_{841}/A_{973}.

Calculation of orientation parameters of polarized infra-red data[29]

Due to the uniaxial orientation nature of annealed iPP fibers arising from cylindrical symmetry, the calculation of orientation parameters obtained from the infra-red data analysis can be carried out using the dichroic ratio (D) defined in the eq. (3):

$$D = A_{\parallel}/A_{\perp} \quad (3)$$

where $A_{\parallel}$ and $A_{\perp}$ are the measured absorbance values for radiation polarized parallel and perpendicular to

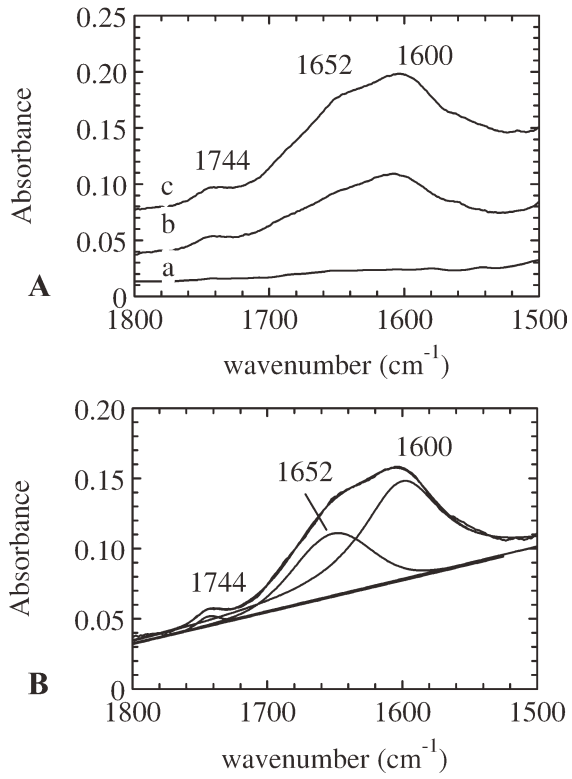

Figure 1 A: Infrared-spectra of isotactic polypropylene fibers in the 1800–1500 cm^{-1} region. (a) unannealed sample; (b) annealed in air at 120°C for 1 h; and (c) annealed in air at 120°C for 3 h. B: Curve fitting of infrared spectrum of isotactic polypropylene fiber annealed in air at 120°C for 3 h (1800–1500 cm^{-1} region).

the fiber axis, respectively. In this work, it is assumed that the PP chains have no preferred orientation around their own axis. The $<P_2(\cos\theta)>$ is known as the second-order Legendre polynomial and is also known as the Herman's orientation factor in the polymer and fiber science. To a good approximation, the dichroic ratio is related to the orientation parameter, $<P_2(\cos\theta)>$, by

$$<P_{200}> = <P_2(\cos\theta)> = \frac{D-1}{D+2}\cdot\frac{2}{(3.\cos^2\alpha - 1)} \quad (4)$$

where θ is the angle between the local chain axis and the fiber axis, and α is the transition moment angle between the associated vibrational mode and the chain axis.

RESULTS AND DISCUSSION

Infra-red spectroscopy measurements

Infrared spectroscopy was found to be useful for monitoring the effects of annealing in air and in glycerine environments, respectively. Detailed analysis of the infrared spectrum of annealed samples showed clear evidence of surface oxidation as shown by the appearance of oxygen containing functional groups on the surface of the samples. The appearance of carbonyl (—C=O) and hydroxyl (-OH) groups in the 1900–1500 cm^{-1} and 3800–3000 cm^{-1} regions indicated the occurrence of oxidation reactions during the annealing treatment. The peaks involved in the carbonyl and hydroxyl regions appeared to be fairly broad in terms of peak breadth and are believed to be due to different oxidation products.

Infrared spectrum of the sample annealed in air in the 1800–1500 cm^{-1} region (Fig. 1) showed clear evidence of oxidation as indicated by the presence of oxygen containing functional groups in comparison with the unannealed sample [Fig. 1(a)]. This region of the infrared spectrum shown in Figure 1(b) was resolved into three peaks at 1744, 1652, and 1600 cm^{-1}, respectively. The band at 1744 cm^{-1} has been attributed to carbonyl (C=O) stretching vibration arising from the presence of ketone, carboxylic acid, and ester groups. The other band at 1652 cm^{-1} may be assigned to double bonded C=C groups conjugated with themselves or with carbonyl groups.[30]

The presence of conjugated C=C groups was indicated by the presence of the IR band at 1600 cm^{-1}. The position of this peak was found to vary between

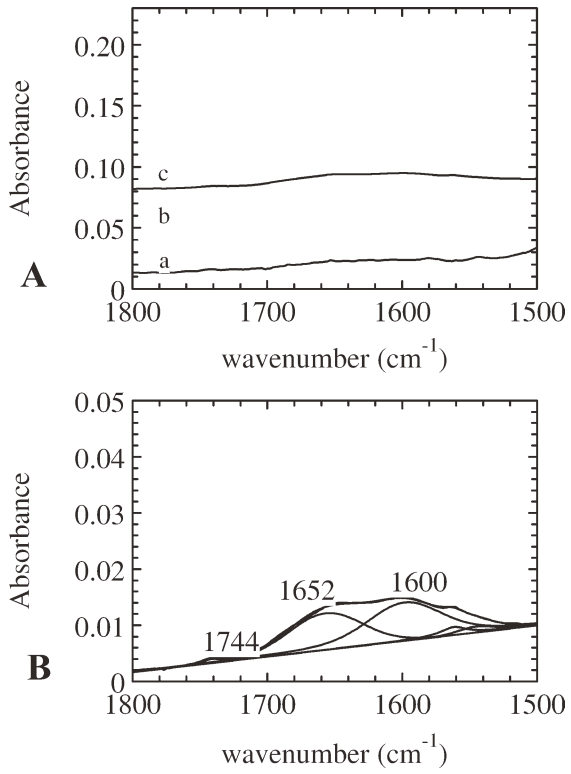

Figure 2 A: Infrared-spectra of isotactic polypropylene fibers in the 1800–1500 cm^{-1} region. (a) unannealed sample; (b) annealed in glycerine at 120°C for 1 h; and (c) annealed in air at 120°C for 3 h. B: Curve fitting of infrared spectrum of isotactic polypropylene fiber annealed in glycerine at 120°C for 3 h in the 1800–1500 cm^{-1} region.

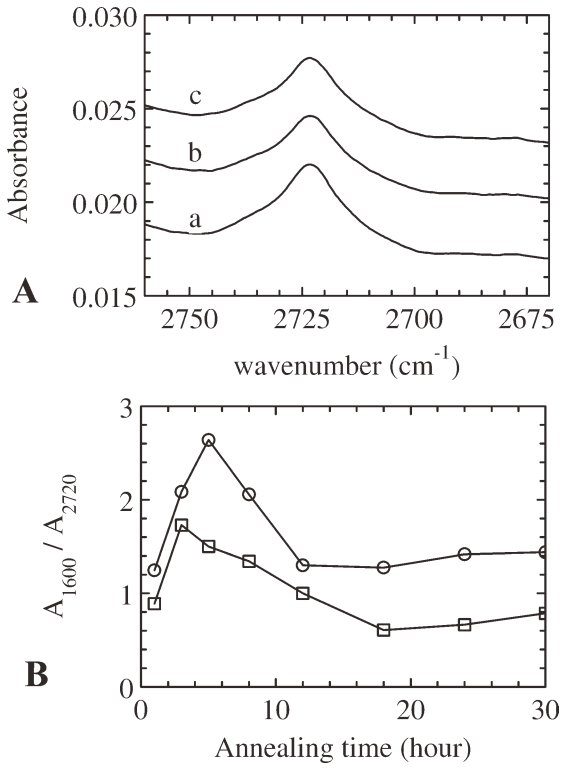

Figure 3 A: Infrared-spectra of isotactic polypropylene fibers annealed in air at 120°C for (a) 1 h; (b) 3 h; and (c) 5 h in the 2760–2670 cm^{-1} region. B: Comparison of absorbance ratio, A_{1600}/A_{2720} of isotactic polypropylene fiber annealed in air (○) and in glycerine (□) at 120°C for 3 h in the 1800–1500 cm^{-1} region.

1595 and 1600 cm^{-1}. The infrared spectra of the glycerine treated samples in the 1800–1500 cm^{-1} region can also be resolved into three bands with similar peak positions (Fig. 2). In the present investigation, to normalize the peak intensities in the 1800–1500 cm^{-1} region, 2720 cm^{-1} peak was used as an internal standard due to its presence in the IR spectrum of melted polymer.[31,32] This peak is assigned to CH bending and CH_3 stretching vibrations[32] and is known to arise from an amorphous phase and is not expected to be sensitive to crystallization effects.[32] Although the intensity of the peak at 2720 cm^{-1} is not very strong, it is not overlapped with the neighboring peaks [Fig. 3(a)].

Since the intensity of the band at 1744 cm^{-1} shown in Figure 1 was too weak for a reliable estimation of the carbonyl content, the absorbance ratio between the 1600 cm^{-1} and 2720 cm^{-1} was used for the evaluation of the conjugated C=C content [Fig. 3(b)]. It can be seen in Figure 1 that the concentration of conjugated C=C groups appears to be higher in the samples annealed in air than in glycerine environments [Fig. 3(b)]. This may be due to the higher conjugation reactions which are likely to occur in the presence of oxygen rich environment than in glycerin environment where less exposure to oxygen and less oxygen uptake is expected to take place.

Infrared spectrum in the 3650–3050 cm^{-1} region is known to mainly contain hydroxyl (-OH) group vibrations[32] [Fig. 4(a)]. This region clearly showed the presence of hydroxyl group vibrations which can be resolved into nine peaks [Fig. 4(b)] at 3500, 3460, 3420, 3370, 3340, 3283, 3201, 3147, and 3116 cm^{-1}, respectively. The results obtained from curve fitting results suggested that the hydroxyl content was slightly higher in annealing carried out in air than in glycerine environment (Fig. 5) where less exposure to oxygen takes place.

Infrared spectrum of annealed iPP fiber was utilized for the determination of the degree of crystalinity. The degree of crystallinity of annealed iPP fibers was evaluated using the absorbance ratios[33,34] of A_{998}/A_{973} and A_{841}/A_{973}. The IR band at 973 cm^{-1} was used as an internal standard[28,35] due to the fact that the intensity of this band is relatively stable, unaffected, and insensitive to the structural changes taking place during the annealing process. 841 and 998 cm^{-1} absorption bands are usually assigned to the crystalline phase, whereas 973 cm^{-1} band is assigned to both crystalline and amorphous chains

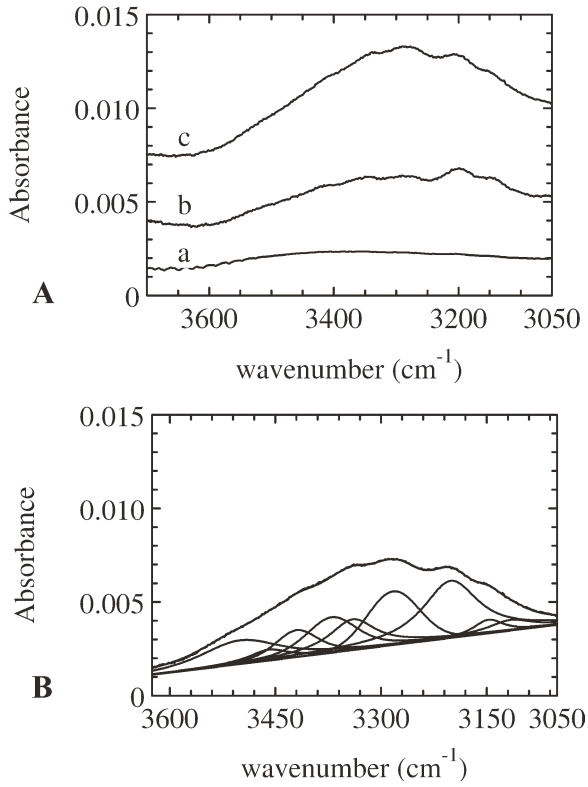

Figure 4 A: Infrared-spectra of isotactic polypropylene fibers (a) unannealed sample; (b) annealed in air at 120°C for 1 h; (c) annealed in air at 120°C for 3 h in the 3625–3050 cm^{-1} region. B: Curve fitting of infrared spectrum of isotactic polypropylene fiber annealed in air at 120°C for 3 h in the 3625–3050 cm^{-1} region.

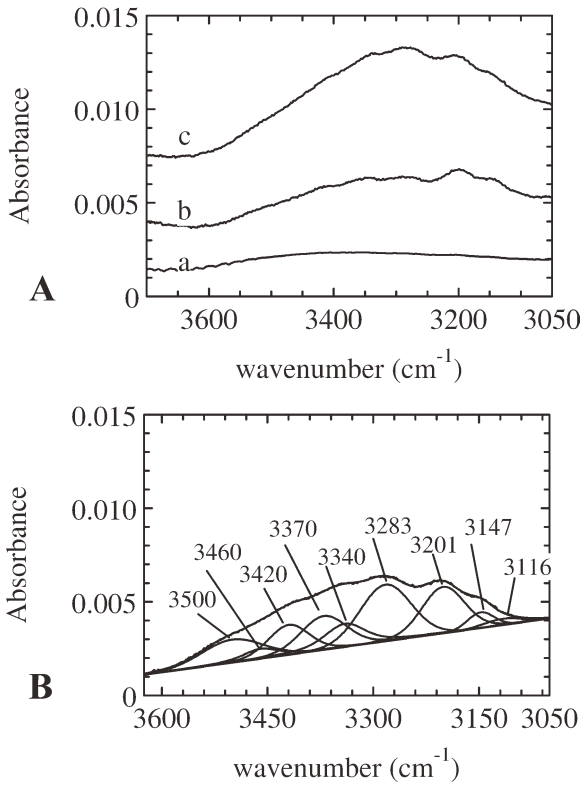

Figure 5 A: Infrared-spectra of isotactic polypropylene fibers (a) unannealed sample; (b) annealed in glycerine at 120°C for 1 h; (c) annealed in glycerine at 120°C for 3 h in the 3625–3050 cm^{-1} region. B: Curve fitting of infrared spectrum of isotactic polypropylene fiber annealed in glycerine at 120°C for 3 h in the 3625–3050 cm^{-1} region.

in helical conformations. 973 cm^{-1} band is associated with the presence of short isotactic helices apparently still present in the melt or in the atactic material.[28]

998 cm^{-1} band is assigned to CH_3 rocking + CH_2 wagging + CH bending vibrations, whereas 973 cm^{-1} belongs to strongly coupled CH_3 rocking + C—C chain stretch vibrations (Table I).[36] The existence of ordered helical chain segments in the melt was shown by Zerbi et al.[37] The spectrum of molten PP showed the existence of a weak band at 998 cm^{-1} indicating that during the melting process not all the helices are destroyed. On melting, this peak drastically lost its intensity but did not completely disappear altogether. It shows that certain proportion of segments of helical structure still exists in the molten phase. The length of these segments is thought to be at least five propylene units in the melt.

It was also confirmed[38] that the band at 998 cm^{-1} still exists at a temperature of 220°C being at least 60°C above the melting point. It was once again shown that a small fraction of ordered helical chain segments still exists in the melt. It was found that the intensity of 998 cm^{-1} band disappears as the sequence length of PP becomes less than 10 monomeric units.[39] The other crystalline band at 841 cm^{-1} is assigned to a combination of CH_2 rocking and C—CH_3 stretching vibrations[40] and shows the lowest peak width in comparison with the other peaks. This peak has an average half-height width of 5.5 cm^{-1}. It has also been assigned to long helical chains with an average length of 12–14 units.[40]

IR crystallinity measurements were carried out after obtaining accurate peak parameters using the curve fitting procedure. Curve fitting was performed in the 1025–775 cm^{-1} region. The calculated IR crystallinity values for the samples annealed in glycerine environment as a function of annealing time are presented in Figure 6. The results suggested that the IR crystallinity values obtained using the absorbance ratio of A_{841}/A_{973} was always higher than that of the absorbance ratio of A_{998}/A_{973} for the samples annealed in glycerine environment. This may possibly be due to the absorption band at 998 cm^{-1} being slightly sensitive to less highly ordered phase. The

TABLE I
Assignment of Polypropylene Infrared Absorption Bands[36] in the 1400–800 cm^{-1} Spectral Region

Frequency (cm^{-1})	Phase	Polarization	Assignment
1377	A,C	⊥	CH_3 symmetric bending + CH_2 wagging
1256	A,C	∥	CH bending + CH_2 twisting + CH_3 rocking
1220	C	⊥	CH_2 twisting + CH bending + C—C chain stretching
1168	C	∥	C—C chain stretching + CH_3 rocking + CH bending
1104	C	⊥	C—C chain stretching + CH_3 rocking + CH_2 wagging + CH twisting + CH bending
1044	C	∥	C—CH_3 stretching + C—C chain stretching + C—H bending
998	C	∥	CH_3 rocking+CH_2 wagging + CH bending
973	A,C	∥	CH_3 rocking + C—C chain stretch
941	C	⊥	CH_3 rocking + C—C chain stretch
900	C	⊥	CH_3 rocking + CH_2 rocking + CH bending
841	C	∥	CH_2 rocking + C—CH_3 stretching
809	C	⊥	CH_2 rocking + C—C stretching + C—H stretching

C, crystalline; A, amorphous.

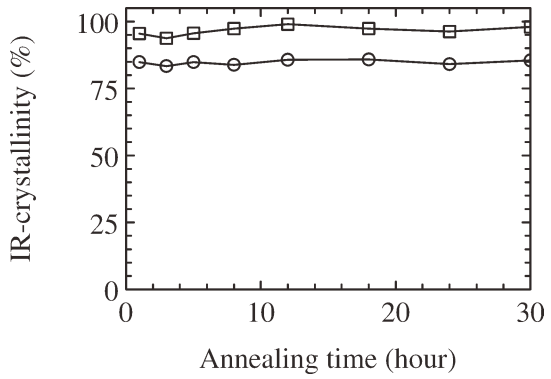

Figure 6 Comparison of IR-crystallinity of isotactic polypropylene fibers annealed in glycerine at 120°C as a function of annealing time. (□) A_{841}/A_{973}; (○) A_{998}/A_{973}.

results showed that there was no clear cut and distinct difference between the crystallinity values obtained from infrared spectroscopy in air and in glycerine environments.

Molecular orientation measurements by polarized infrared spectroscopy

An assessment of the molecular orientation parameters was carried out from an analysis of polarized infrared spectroscopy of iPP fibers annealed in air and in glycerine environments at 120°C for annealing times ranging from 1 to 30 h. In the published literature, the IR bands located at 998, 899, 841, and 809 cm^{-1} are often regarded as characteristic regularity bands arising from the presence of helical chains.[40] Infrared spectrum of amorphous PP shows the intensity of the regularity bands as being very weak or totally absent. The behavior of the regularity bands in the polarized infrared spectroscopy should throw some light on the possible molecular changes which take place during the annealing process.

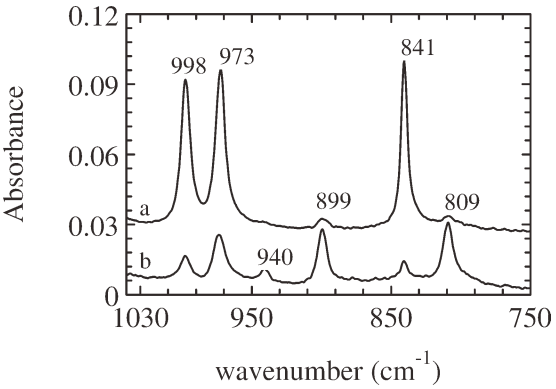

Figure 7 Polarized infrared spectra of isotactic polypropylene fibers annealed in glycerine at 120°C for 1 h. (a) polarization vector parallel to the fiber axis; (b) polarization vector perpendicular to the fiber axis.

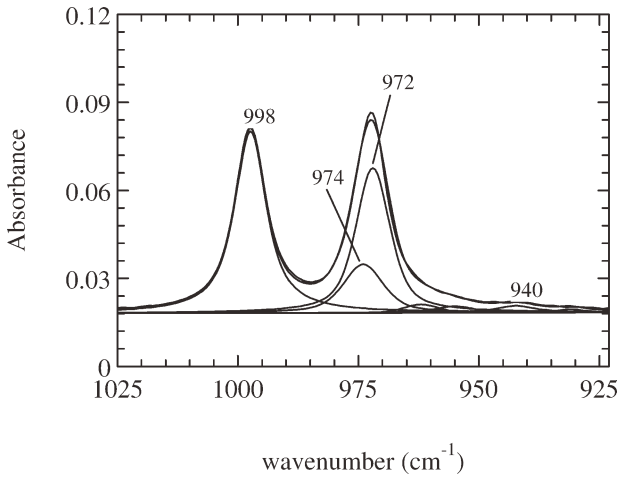

Figure 8 Curve fitting of the polarized infra-red spectrum of isotactic polypropylene fiber annealed in glycerine at 120°C for 1 h in the 1025–923 cm^{-1} range. Polarization vector is parallel to the fiber axis direction.

Figure 7 shows the polarization directions of the regularity peaks (998, 899, 841, and 809 cm^{-1}) in the 1025–775 cm^{-1} spectral region. Most often, the IR bands located at 998, 973, and 841 cm^{-1} are used for the evaluation of the crystalline and average orientation parameters.[41] The IR bands at 998, 973, and 841 cm^{-1} show parallel polarization characteristics whereas the IR bands located at 940, 899, and 809 cm^{-1} show perpendicular polarization characteristics (Fig. 7). The orientation parameters calculated using the regularity band at 841 cm^{-1} for iPP films showed good agreement and correlation with the X-ray diffraction measurements.[41] It was suggested that in the absence of X-ray diffraction data, this peak may be used for the determination of the crystalline orientation parameter. The IR band at 841 cm^{-1} was assigned to long and regular helical chains, most of which are likely to be present in the crystalline regions.[39]

To determine the orientation parameter ($<P_2>$), in the first stage, infrared spectrum in the 1025–725 cm^{-1} region was resolved into six peaks located at 809, 841, 899, 940, 973, and 998 cm^{-1}. From this curve fitting, accurate peak parameters for the bands at 998, 973, and 841 cm^{-1} were obtained and used in the evaluation of the orientation parameter, $<P_2>$ using the eqs. (3) and (4). Transition moment angle (α) for these peaks was taken as zero degree.[42] In the second stage of the analysis, the band at 973 cm^{-1} was separated into the 972 cm^{-1} component assigned to the crystalline phase and the 974 cm^{-1} component assigned to the amorphous phase using the curve fitting procedure detailed earlier in the 1025–923 cm^{-1} spectral range (Fig. 8). The band at 974 cm^{-1} was used for the evaluation of the orientation parameter of the amorphous phase. Even though the IR band at 973 cm^{-1} was separated into

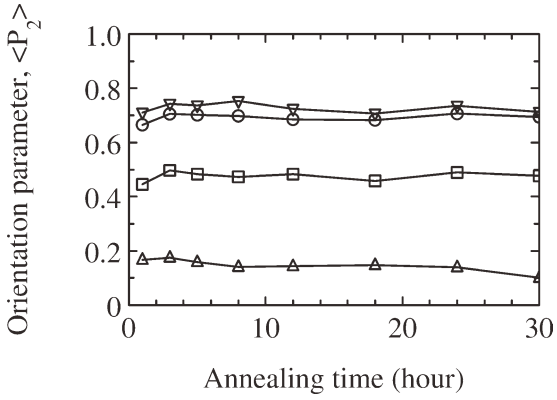

Figure 9 Comparison of orientation parameters, $<P_2>$, obtained from isotactic polypropylene fibers annealed in glycerine at 120°C as a function of annealing time. (▽, 841 cm^{-1}; ○, 998 cm^{-1}; □, 973 cm^{-1}; Δ, 974 cm^{-1}).

two bands, it was assumed that both of these bands were due to the same vibrational mode.[41]

Painter et al.[43] showed using difference spectroscopy that the 972 cm^{-1} peak is attributable to the ordered structure and the 974 cm^{-1} peak is attributable to the disordered structure. Figure 9 shows the comparison of the orientation parameter, $<P_2>$, obtained from iPP fibers annealed in glycerine at 120°C as a function of annealing time for the IR bands located at 998, 973, 974, and 841 cm^{-1}. The results presented in Figure 9 showed that the values of the orientation parameter corresponding to the crystalline phase arising from the dichroic behavior of the peaks at 998 and 841 cm^{-1}, showed a rise between the annealing times of 1 and 3 h followed by a monotonous continuation without much change in the values of the orientation parameters until the annealing time of 24 h, after which a small decline in the orientation parameter occurred until the annealing time of 30 h. The decline in molecular orientation may be due to the effect of structural degradation mechanism making its presence felt after prolonged annealing times.

The values of the orientation parameter, $<P_2>$, obtained from the 998, 974, and 973 cm^{-1} peaks were found to be lower than those obtained from the 841 cm^{-1} peak as a function of annealing time (Fig. 9). Figure 10(a) shows a comparison of the values of the orientation parameter ($<P_2>$) obtained from the 841 cm^{-1} and 998/973 cm^{-1} infrared peaks for the samples annealed in air and in glycerine environments. The values of the orientation parameter corresponding to the 973 cm^{-1} peak assigned to the average phase obtained from the samples annealed in air and in glycerine environments were found to be significantly lower than those obtained from the IR bands at 998 and 841 cm^{-1} [Fig. 10(a)]. It is clear that there was no distinct difference between the orientation parameters obtained from the samples annealed in air and in glycerine environments.

Figure 10(b) shows the comparison of the values of the orientation parameter ($<P_2>$) obtained from the 998 cm^{-1} infra-red peak against those obtained from the 972 cm^{-1}, 973 cm^{-1}, and 974 cm^{-1} infra-red peaks for the samples annealed in air and in glycerine environments. The orientation behavior of the 972 cm^{-1} peak was found to be similar to that of the 998 cm^{-1} peak for the samples annealed in both air and in glycerine environments. The 974 cm^{-1} peak was assigned to the amorphous phase and the values of the orientation parameters obtained from this peak were found to be lower than those obtained from the 972 cm^{-1} peak attributed to the

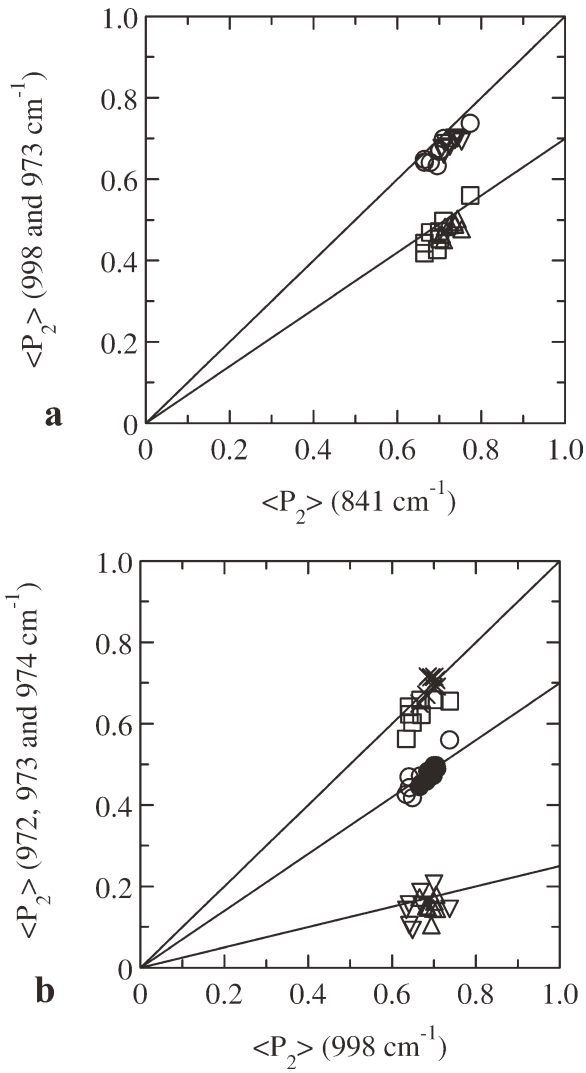

Figure 10 (a) Comparison of the values of the orientation parameter ($<P_2>$) obtained from the 841 cm^{-1} and 998/973 cm^{-1} infrared peaks: annealed in air, 998 cm^{-1} (○); and 973 cm^{-1} (□). Annealed in glycerine, 998 cm^{-1} (Δ); and 973 cm^{-1} (▽). (b) Comparison of the values of the orientation parameter ($<P_2>$) obtained from the 998 cm^{-1} infra-red peak with those obtained from the 972 cm^{-1}, 973 cm^{-1} and 974 cm^{-1} infra-red peaks. Annealed in air, 972 cm^{-1} (□); 973 (○), and 974 cm^{-1} (▽). Annealed in glycerine, 972 cm^{-1} (×); 973 (●), and 974 cm^{-1} (Δ).

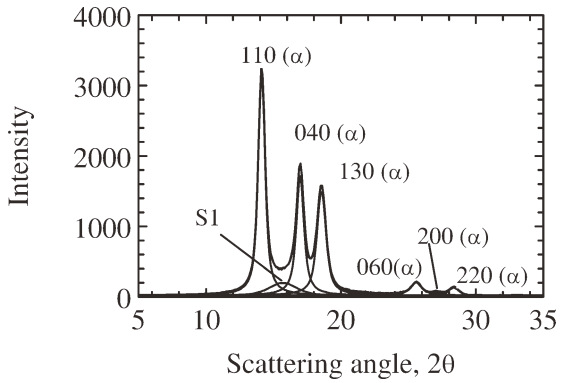

Figure 11 Curve fitting of equatorial X-ray diffraction trace of isotactic polypropylene fiber annealed in glycerine at 120°C for 1 h.

crystalline phase and the 973 cm^{-1} peak attributed to the average phase for the samples annealed in both air and glycerine environments.

It should be noted that during the assessment of the orientation parameter obtained from the polarized infrared spectroscopy approach, the semicrystalline polymer structure was assumed to be due to the presence of only crystalline and amorphous phases, respectively. No consideration was given for the presence of paracrystalline (smectic) phase. This was mainly attributed to the difficulties of separation of the infrared bands due to the crystalline and smectic structures.

X-ray diffraction measurements

Due to its sensitivity to ordered regions, X-ray diffraction method is routinely used to determine the degree of crystallinity and the apparent crystallite size of samples with some degree of order. In the present investigation, following the curve fitting procedure, equatorial X-ray diffraction traces were used to obtain the degree of apparent crystallinity and the apparent crystallite size of the corresponding crystalline reflections for the iPP fibers annealed in air and in glycerine environments at an annealing temperature of 120°C and annealing times ranging from 1 to 30 h.

During the course of the present investigation, curve fitting procedure was extensively utilized to obtain accurate peak parameters in terms of peak positions, peak heights, and half-height widths. A typical curve fitting for the sample annealed in glycerine environment at 120°C for 1 h is shown in Figure 11 together with the peak parameters including the comparison of the observed and calculated *d*-spacings are listed in Table II.

A typical equatorial X-ray diffraction trace of annealed as-spun fiber presented in Figure 11 showed three strong [(110), (040), and (130)] and well defined reflections together with three weak reflections [(060), (200), and (220)]. The crystalline structure shown in Figure 11 exhibits a characteristic α-monoclinic structure. Equatorial X-ray diffraction trace shown in Figure 11 was fitted with six crystalline peaks indexed as 110, 040, 130, 060, 200, and 220, respectively. It was necessary to use an additional peak located at $2\theta = 15.71°$ (*d*-spacing of 0.564 nm) during the curve fitting stage to enhance the fitting in the tail regions of the neighboring peaks. The half-height width of this peak is relatively broad and exhibits the typical characteristic of a paracrystalline (or smectic) phase.[2–4,44,45]

It has been reported in the published literature that the smectic phase of iPP is quite stable at room temperature for long periods but transforms to the more stable α-monoclinic structure on heating to temperatures above 60°C.[46–48] The smectic phase is known to show a typical behavior of an intermediate order between the crystalline and the amorphous phase.[46–48] In the smectic phase, propylene units are known to form helical chain conformations and are usually found to be arranged parallel to each other on a local scale with little or no lateral register while exhibiting no long range order. It has been reported that the X-ray diffraction traces of iPP produced from rapidly quenched melt incorporating smectic phase contains two broad peaks with peak positions of $2\theta = 15.71°$ (*d*-spacing of 0.564 nm) and $2\theta = 22°$ (*d*-spacing of 0.4 nm), respectively. The peak located at $2\theta = 15.71°$ is related to the average interchain distance between adjacent chains in the smectic

TABLE II
Peak Parameters of Curve Fitted Equatorial X-ray Diffraction Trace of Isotactic Polypropylene Fiber Annealed in Glycerine at 120°C for 1 h

Peak ref.	*f*	*A* (Height)	HHW (Width)	Position (2θ)	*d*-obs spacing (nm)	*d*-calc spacing (nm)
α-110	0.37	3179.0	0.666	14.1269	0.626	0.626
S-1	0.65	176.0	2.780	15.705	0.564	–
α-040	0.21	1702.5	0.710	16.9723	0.522	0.522
α-130	0.31	1484.0	0.843	18.5569	0.478	0.478
α-060	0.0	183.5	0.999	25.5686	0.348	0.348
α-200	1.0	40.2	0.840	27.123	0.328	0.328
α-220	1.0	107.2	1.090	28.3532	0.314	0.313

HHW, half-height width.

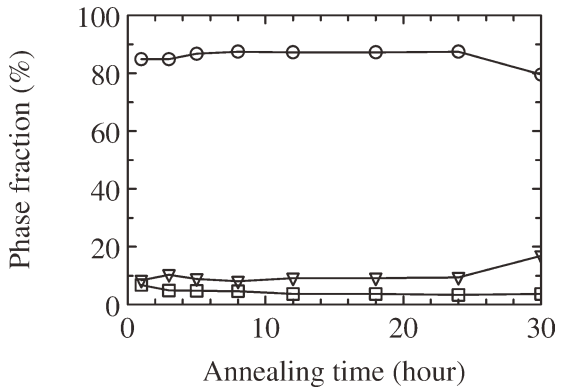

Figure 12 Comparison of α, smectic, and amorphous phase fractions obtained from an analysis of the equatorial X-ray diffraction traces of isotactic polypropylene fibers annealed in glycerine at 120°C as a function of annealing time. (○) α-phase, (□) smectic phase, and (▽) amorphous phase.

phase and is not related to stereoregularity (or tacticity) of the polymer chains.[49]

The 2nd peak with a *d*-spacing of 0.4 nm seems to disappear from the equatorial traces and is reported to move to the first layer line (*hk1*, $l = 1$) when a highly oriented and drawn sample is produced.[50] This is the main reason why only one peak with a *d*-spacing of 0.564 nm ($2\theta = 15.7°$) was used during the curve fitting stage of the equatorial X-ray diffraction traces of the annealed fiber samples under investigation.

Evaluation of the apparent X-ray crystallinity

By definition, X-ray diffraction method is most sensitive to the ordered material and measures the relative proportion of the ordered material. X-ray diffraction method is routinely used as a reliable method of measuring crystallinity. X-ray crystallinity can be viewed as a measure of the lateral order due to the use of equatorial diffraction traces after the curve fitting procedure. For this reason, the term "apparent crystallinity" should be used instead of the "crystallinity" implying absolute crystallinity.

TABLE III
Comparison of α-, Smectic, and Amorphous Phase Fractions Obtained from an Analysis of the Equatorial X-ray Diffraction Traces of Isotactic Polypropylene Fibers Annealed in Glycerine Environment at 120°C as a Function of Annealing Time

Annealing time (h)	α-phase (%)	Smectic (%)	Amorphous (%)
1	84.8	6.8	8.4
3	84.8	4.9	10.3
5	86.8	4.7	8.9
8	87.4	4.6	8.0
12	87.2	3.7	9.1
18	87.2	3.7	9.1
24	87.4	3.3	9.3
30	79.5	3.7	16.8

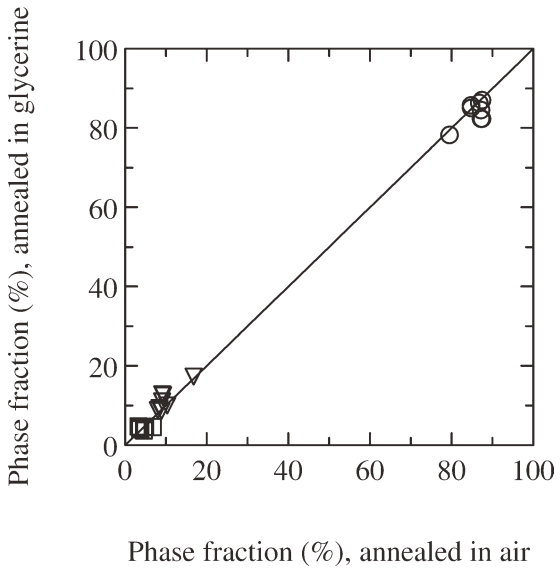

Figure 13 Comparison of the phase fractions of isotactic polypropylene fibers annealed at 120°C in glycerine and in air environments obtained from an analysis of the equatorial X-ray diffraction traces. (○) α-phase, (□) smectic phase, and (▽) amorphous phase.

Apparent crystallinity values due to α-monoclinic phase increased continuously with increasing annealing time up to 24 h and showed a decline when the annealing time of 30 h was reached (Fig. 12). Annealing in glycerine resulted in α-monoclinic phase fractions varying between 80 and 87%, whereas amorphous phase varied between 8 and 17% (Table III). Smectic phase fraction due to the annealing in glycerine environment decreased even below amorphous phase fraction and was found to decline from 7 to 3% between the annealing times of 1 and 30 h. It is clear that the smectic phase was not completely transformed to the α-monoclinic phase.

The results undoubtedly showed that there was a direct relationship between the structural transformation and the annealing treatment during which less stable smectic form was transformed to a more stable α-monoclinic form as a function of annealing time whether the samples were annealed in air or in glycerine environments. It was shown that annealing in air and in glycerine environments resulted in an enhanced degree of α-phase crystallinity at the expense of the smectic phase structure. The results showed that there was no significant difference between the apparent X-ray crystallinity values measured for the samples annealed in air and in glycerine environments (Fig. 13).

Evaluation of the apparent crystallite sizes

During the evaluation of apparent crystallite size calculations, the broadening imposed by the finite width of the X-ray diffractometer beam was taken

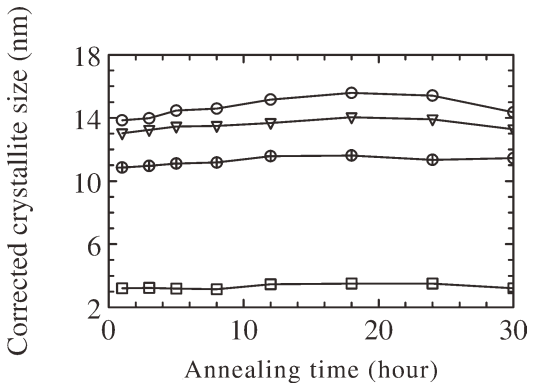

Figure 14 Comparison of the apparent crystallite size of isotactic polypropylene fibers annealed in glycerine at 120°C as a function of annealing time. (○) 110; (▽) 040; (●) 130, and (□) smectic peak.

into account. In the present investigation, the correction of the half-height widths was performed using Stoke's deconvolution method.[27] In the first stage, observed half-height widths were corrected for the instrumental effects. In the second stage, corrected half-heights were used for the calculation of the corrected crystallite sizes for the relevant peaks using the Scherrer's equation [eq. (2)] arising from the

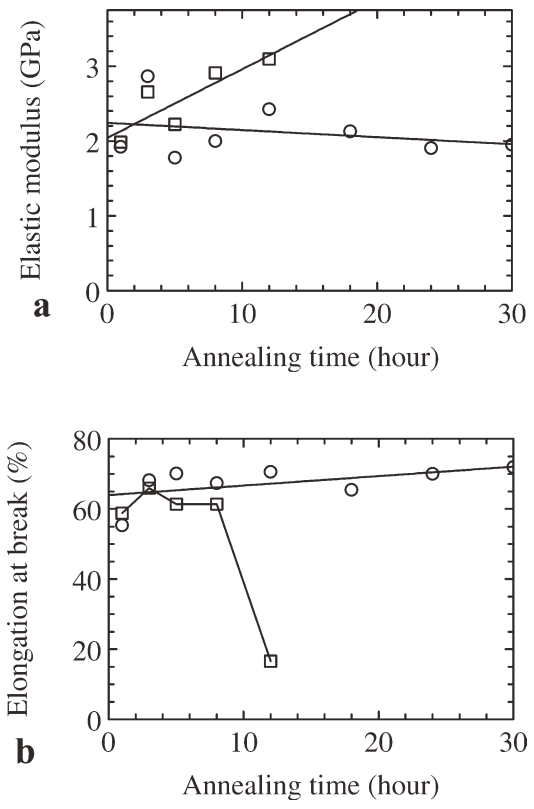

Figure 15 Comparison of elastic modulus (a) and elongation at break (b) values of isotactic polypropylene fibers annealed in air (□) and in glycerine (○) environments at 120°C as a function of annealing time.

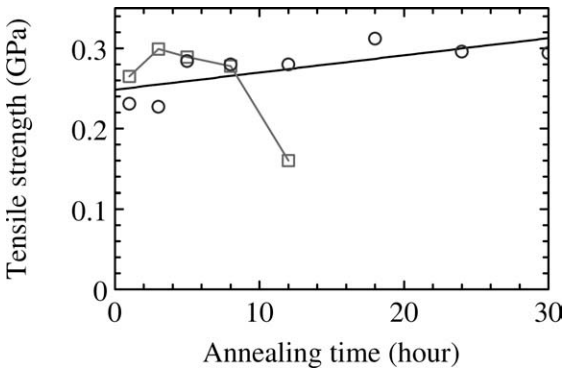

Figure 16 Comparison of tensile strength values of isotactic poolypropylene fibers annealed in air (□) and in glycerine (○) environments at 120°C as a function of annealing time.

presence of α-monoclinic and smectic forms in the annealed structures.

Figure 14 shows the comparison of the apparent crystallite size of isotactic polypropylene fibers annealed in glycerine at 120°C as a function of annealing time. It was shown that the (110) reflection characterized as a very sharp peak in the equatorial X-ray diffraction trace resulted in the highest crystallite size in comparison with the (040) and (130) peaks. As shown in Figure 14, the apparent crystallite size corresponding to the (110) reflection was higher than that of the (040) and (130) reflections. The apparent size due to the smectic phase was the lowest in comparison with the α-monoclinic phase reflections of (110), (040), and (130), respectively. The results suggested that there was no clear cut and distinct difference between the apparent crystallite sizes obtained from annealing in air and in glycerine environments.

Assessment of the mechanical properties

Evaluation of the mechanical properties of the fibers can be regarded as a very important characteristic which influence the behavior of fibers during the processing and the performance of the final product.[51] The samples annealed in air at 18, 24, and 30 h were so degraded that the mechanical property measurements could not be carried out due to the loss of the fiber form. The loss of fiber form may be due to the excessive oxygen uptake occurred during the annealing in air and the chain scission related loss of mechanical properties. The samples annealed in the glycerine environment did not lose the physical form and all the mechanical property measurements were carried out with success.

Figure 15(a) shows the comparison of elastic modulus values of isotactic polypropylene fibers annealed in air and in glycerine environments at 120°C as a function of annealing time. Elastic

modulus values measured for the samples annealed in air showed an upward trend until the annealing time of 12 h whereas those samples annealed in glycerine environment showed downward trend between the annealing times of 1 and 30 h. Elongation at break values measured for the samples annealed in air showed a gradual decrease until the annealing time of 12 h with increasing annealing time, whereas the measured values for the samples annealed in glycerine environment showed a gradual and continuous increase with increasing annealing time [Fig. 15(b)].

Although there is large data scatter, tensile strength values of the samples annealed in glycerine environment presented in Figure 16 showed an increase with increasing annealing time whereas the values of the tensile strength for the samples annealed in air showed a continuous decline up to the annealing time of 12 h, afterwards the samples lost their physical form due to the excessive degradation. The decrease in the tensile strength between the annealing times of 1 and 12 h may be due to an oxidation related thermal degradation which may have caused considerable amount of chain scission and the eventual loss of tensile strength.

CONCLUSIONS

Dry and wet annealing treatment of isotactic polypropylene fibers was carried out in air and in glycerine environments under constant length at an annealing temperature of 120°C with annealing times varying from 1 to 30 h. A close examination of the results obtained from the infrared spectrum of the samples annealed, especially in air, showed clear evidence of the surface oxidation as indicated by the presence of hydroxyl and carbonyl groups on the surfaces of the samples. The results showed an improvement in the structural parameters as shown by the crystallinity, crystallite size, and the orientation measurements obtained from X-ray diffraction and infrared spectroscopy methods. Data obtained from the X-ray diffraction measurements showed a transformation of smectic phase to a α-monoclinic phase with increasing annealing time. Crystallinity, crystallite size, and orientation measurements carried out for the samples annealed in air and in glycerine environments showed no clear cut difference.

Mechanical properties of the samples annealed in air and in glycerine environments were affected to a certain extent. Annealing in air resulted in an excessive degradation and led to the loss of tensile strength up to the annealing time of 12 h due to an oxidation related chain scission mechanism whereas annealing in glycerine environment resulted in an increase of the tensile strength without loss of physical form up to the annealing time of 30 h. It is clear that wet annealing in glycerine environment rather than in air is useful to obtain enhanced tensile strength values.

The assistance and cooperation of Boyteks A.Ş. (Kayseri) is gratefuly acknowledged for the extrusion of the polypropylene multifilaments.

References

1. Samuels, R. J. Structured Polymer Properties; Wiley: New York, NY, USA, 1974.
2. Sheehan, W. C.; Cole T. B. J Appl Polym Sci 1964, 8, 2359.
3. Wang, I. C.; Dobb, M. G.; Tomka, J. G. J Text Inst 1995, 86, 383.
4. Wang, I. C.; Dobb, M. G.; Tomka J. G. J Text Inst 1996, 87, 1.
5. Nadella, H. P.; Henson, H. M.; Spruiell, J. E.; White, J. L. J Appl Polym Sci 1977, 21, 3003.
6. Fung, P. Y. F.; Orlando, E.; Carr, S. H. Polym Eng Sci 1973, 13, 295.
7. Kitao, T.; Ohya, S.; Furukawa, J.; Yamashita, S. J Polym Sci Polym Phys 1973, 11, 1091.
8. Spruiell, J. E.; White, J. L. Polym Eng Sci 1975, 15, 660.
9. Minoshima, W.; White, J. L.; Spruiell, J. E. J Appl Polym Sci 1980, 25, 287.
10. Shimizu, J.; Watanabe, A.; Toriumi, K. Sen-i Gakkaishi 1974, 30, T53.
11. Shimizu, J.; Torid, K.; Tamai, K. Sen-i Gakkaishi 1977, 33, T255.
12. Shimizu, J.; Tonumi, K.; Imai, Y. Sen-i Gakkaishi 1979, 35, T405.
13. Shimizu, J.; Okui, N.; Imai, Y. Sen-i Gakkaishi 1980, 36, T166.
14. Lu, F. M.; Spruiell, J. E. J Appl Polym Sci 1987, 34, 1521.
15. Lu, F. M.; Spruiell, J. E. J Appl Polym Sci 1987, 34, 1541.
16. Minoshima, W.; White, J. L.; Spruiell, J. E. Polym Eng Sci 1980, 20, 1166.
17. Spruiell, J. E.; Lu, F.-M.; Ding, Z.; Richeson, G. J Appl Polym Sci 1965 1996, 62.
18. Gupta, V.B. J Appl Polym Sci 2002, 83, 586.
19. Farrow, G. Polymer 1963, 14, 191.
20. Suzuki, A.; Narusue, S. J Appl Polym Sci 2004, 92, 1534.
21. Suzuki A.; Narusue, S. J Appl Polym Sci 2006, 99, 27.
22. Suzuki, A.; Ohnishi, H. J Appl Polym Sci 2006, 102, 2600.
23. Kunugi, T.; Ito, T.; Hashimoto, M.; Ooishi, M. J Appl Polym Sci 1983, 28, 179.
24. Mukhopadhyay, S.; Deopura, B.L.; Alagirusamy, R. J Text Inst 2005, 96, 349.
25. Hindeleh, A. M.; Johnson, D. J.; Montague, P. E. In Fibre Diffraction Methods; French, A. D., Gardner, K. H., Eds.; ACS Symp. No. 141; American Chem Society: Washington DC, 1983; pp 149–181.
26. Hindeleh, A. M.; Johnson, D. J Polymer 1978, 19, 27.
27. Stokes, A. R. Proc Phys Soc 1948, A166, 382.
28. Tadokoro, H.; Kobayashi, M.; Ukita, M.; Yasufuku, K.; Murahashi, S.; Torii, T. J Chem Phys 1965, 4, 1432.
29. Karacan, I.; Bower, D. I.; Ward, I. M. Polymer 1994, 35, 3411.
30. Rjeb, A.; Tajounte, L.; Chafik El Idrisi, M.; Letarte, S.; Adnot, A.; Roy, D.; Claire, Y.; Perichaud, A.; Kaloustian, J. J Appl Polym Sci 2000, 77, 1742.
31. Mirabella, F.M. J Polym Sci Part B: Polym Phys 1987, 25, 591.
32. Rabello M. S.; White, J. R. Polym Degrad Stab 1997, 56, 55.
33. Huy, T. A.; Adhikari, R.; Lüpke, T.; Henning, S.; Michler, G. H. J Polym Sci Part B: Polym Phys 2004, 42, 4478.
34. Lamberty, G.; Brukato, V. J Polym Sci Part B: Polym Phys 2003, 41, 998.
35. Burfield, D. R.; Loi, P. S. T. J Appl Polym Sci 1988, 36, 279.

36. Jasse, B.; Koenig, J. L. J Macromol Sci-Rev Macromol Chem 1979, C17, 61.
37. Zerbi, G.; Gussoni, M.; Ciampelli, F. Spectrochim Acta Mol Spectrom 1967, 23, 301.
38. Zhu, X.; Yan, D.; Yao, H.; Zhu, P. Macromol Rapid Commun 2000, 21, 354.
39. Kissin, Yu. V.; Tsvetkova, V. I.; Chirkov, N. M. Eur Polym Mater 1972, 8, 529.
40. Kissin, Yu. V.; Rashina L. A. Eur Polym Mater 1976, 12, 757.
41. Karacan, I.; Taraiya, A. K.; Bower, D. I.; Ward, I. M. Polymer 1993, 34, 2691.
42. Gupta, M. K.; Carlsson, D. J.; Wiles, D. M. J Polym Sci Part B: Polym Phys 1984, 22, 1011.
43. Painter, P. C.; Watzek, M.; Koenig, J. L. Polymer 1977, 18, 1169.
44. Miller, R. L. Polymer 1960, 1, 135.
45. Fujiyama, H.; Awaya, H.; Azuma, K. J Polym Sci Polym Lett 1980, 18, 105.
46. Gailey, J. A.; Ralston, R. H. SPE Trans 1964, 4, 29.
47. Corradini, P.; Petroccone, V.; De Rosa, C.; Guerra, G. Macromolecules 1986, 19, 2699.
48. Zanetti, R.; Celotti, G.; Fichera, A.; Francesconi, R. Makromol Chem 1969, 128, 137.
49. O'Kane, W. J.; Young, R. J.; Ryan, A. J.; Bras, W.; Derbyshire, G. E.; Mant, G. R. Polymer 1994, 35, 1352.
50. Poddubny, V. I.; Lavrentyev, V. K.; Sidorovich, A. V.; Baranov, V. G. Acta Polym 1982, 33, 483.
51. Morton, W. E.; Hearle, J. W. S. Physical Properties of Textile Fibres; Butterworth and Co. (Publishers) Ltd. and the Textile Institute, Cambridge, England, 2008.